КОНДЕНСАЦИЯЛАНҒАН КҮЙДІҢ ФИЗИКАСЫ
ФИЗИКА КОНДЕНСИРОВАННОГО СОСТОЯНИЯ
PHYSICS OF THE CONDENSED MATTER

D.A. Afanasyev[1,2], N.Kh. Ibrayev[1], E.Zh. Alikhaidarova[1]

[1]Ye.A. Buketov Karaganda State University, Kazakhstan;
[2]Institute of Applied Mathematics, Kazakhstan
(E-mail: a_d_afanasyev@mail.ru)

Charge transfer and properties of localized plasmon resonance in Ag-TiO$_2$ nanostructures

In the paper the results of the synthesis of Ag – TiO2 nanostructures are presented. Nanostructures consist of a silver core and a TiO$_2$ semiconductor shell. The size of nanostructures (NSs), determined by the method of dynamic light scattering, was 20 nm and 50 nm in different medias. The effect of the semiconductor shell of TiO$_2$ on the properties of the localized plasmon resonance of silver nanoparticles is investigated. The quantitative index of localized plasmon resonance in NSs (electron density) was deteriorated, while the qualitative indicator of localized plasmon resonance (attenuation coefficient of plasma oscillations) can improve in the case of a thin TiO$_2$ shell. After the synthesis of the TiO$_2$ shell an additional luminescence band of the Ag – TiO$_2$ NS is observed. The observed luminescence is associated with charge transfer from TiO$_2$ on Ag. The dependence of the maximum recombination luminescence band on the value of the charge on silver nanoparticles is observed.

Keywords: localized plasmon resonance, silver nanoparticle, nanostructures, charge transfer, titanium dioxide.

Introduction

The number of applied applications of plasmon resonance observed in nanoparticles (NPs) and nanostructures (NSs) of metals increases every year [1]. Compositions of the interrelated components of various substances, one or several of which have linear dimensions in the nanorange are taken to nanostructures. However, the wider practical application of metal NPs and NSs is limited by their chemical activity [2]. This is due to the increase in the specific surface of the particles with a decrease in their size [3]. One of the main ways to protect NPs from destruction is the synthesis of the protective shell. A schematic plot of the core-shell NS and their main geometrical parameters are shown in Figure 1. The shell can be from both organic and inorganic materials. The most commonly used substances are oxide materials, such as TiO$_2$ and SiO$_2$ [1]. They are highly stable. Core-shell nanostructures can be used for photocatalysis, in medicine, electronics and photovoltaics [4–6]. An important positive quality of NS core-shell is the ability to change the characteristics of the resulting nanoparticles. In particular, it is possible to change the characteristics of localized plasmon resonance (LPR) of metal nanoparticles.
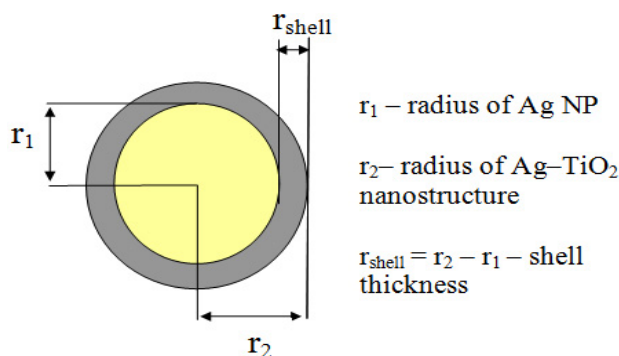
Figure 1. Schematic plot of Ag-TiO$_2$ nanostructures

Also for core-shell NSs can be observed that weren't observed for metals NPs. One such effect is charge transfer across the semiconductor/metal interface. Charge transfer can occur both from a metal nanoparticle to semiconductor when LPR is excited in it [7] and from TiO$_2$ when a semiconductor absorbs light and electrons transfer to the conduction band of silver [8]. If a large amount of work is devoted to charge transfer from metal to semiconductor, then the process of charge transfer from TiO$_2$ to metal is few understood.

The aim of the present work was to study the charge transfer process in nanostructures of the «plasmon core-semiconductor shell» and to study the influence of the semiconductor shell on the LPR of silver nanoparticles.

Method of experiment

The method of synthesis of Ag-TiO$_2$ NSs, used in the work, is described in detail in [9]. Originally, silver NPs were synthesized. To reduce the concentration of additional reagents in the solution, the production of silver nanoparticles in water was carried out by laser ablation in a liquid. The setup diagram for the production of nanoparticles and the conditions for carrying out the synthesis are given in [10].

After the synthesis of silver NPs, titanium dioxide semiconductor shells (TiO$_2$) were synthesized. The core-shell nanostructures are synthesized by adding a solution of titanium tetraisopropoxide (TIPT) to an ethanol solution of silver NPs. All of these components are added during vigorous stirring of the solution. During the synthesis, the following ratio between the reagents was mainly chosen: 6 μl of TIPT was added to 1 ml of ethanol. In 10 ml of silver NP solution was added 1 ml of TIPT solution. After this, the reaction mixture is stirred for 12 hours at room temperature in the dark. Also, besides the standard concentration of TIPT, concentrations were used 2 times and 3 times less than the standard (concentrations TIPT of 50 % and 30 % of the standard respectively).

The average sizes of the obtained NPs and NSs were determined by the method of dynamic light scattering on the Zetasizer Nano ZS (Malvern) particle size analyzer. The morphology of the NPs was studied on a Tescan Mira 3 scanning electron microscope (SEM). Absorption spectra were recorded on a Cary 300 spectrophotometer (Agilent), and fluorescence was recorded on an Eclipse spectrofluorometer (Agilent).

Results and its discussion

Originally, silver NPs were synthesized. Their size was r$_1$ ~ 20 nm (Fig. 2, a), r$_1$ as pointed in Figure 1. Then, an Ag-TiO$_2$ NSs with different thicknesses of the semiconductor shell was synthesized in an ethanol solution (r$_{shell}$ in Fig. 1). The obtained TiO$_2$ shell thickness in synthesized NSs was equal to r$_{shell}$=23 nm (Fig. 2, b) and r$_{shell}$=63 nm (Fig. 2, c). The use of NSs with a shell of different thickness will allow you to determine the degree of influence of the semiconductor shell on the properties of decision maker silver NPs. The concentration of NSs in solution was 4,1 * 10^{-8} mol/l. The sizes of NPs and NSs in aqueous solution are shown in Figure 2 and Table.

a)

b)

c)
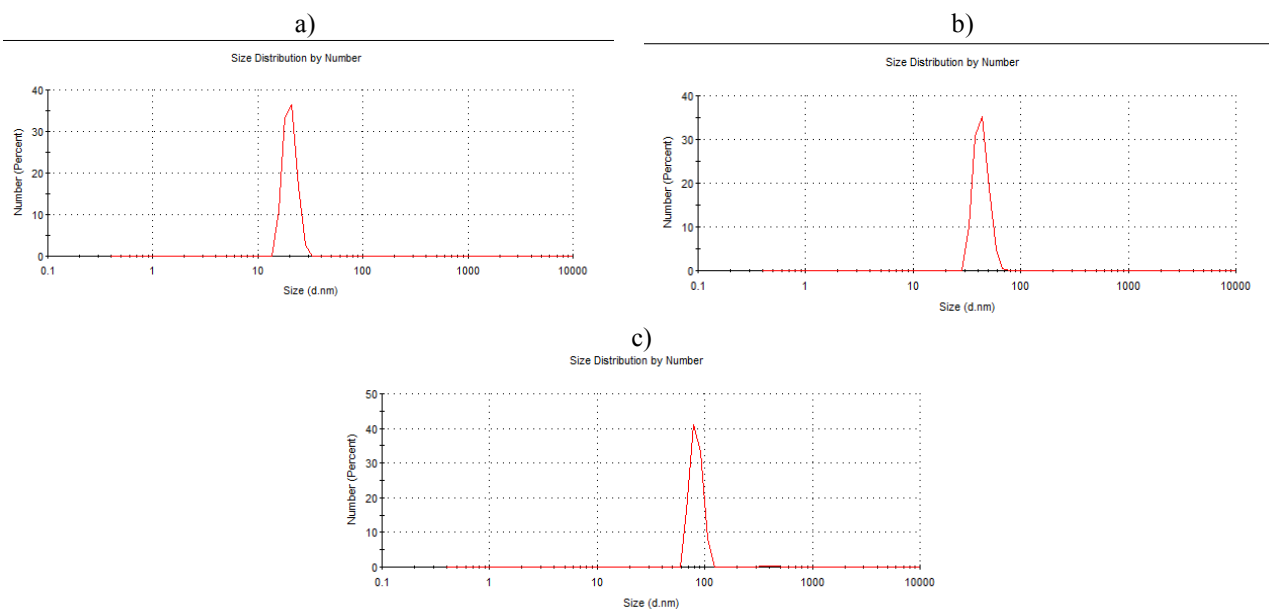
Figure 2. The size distribution of Ag (a) and Ag-TiO$_2$ nanoparticles with
a concentration TIPT of 30 % of the standard (b) and 50 % (c) in water

T a b l e

Size and main characteristics of the absorption spectra of the NSs «plasmon core/semiconductor shell»

Characteristics of solutions NP and NS	Particle size, nm	λ_{abs}^{max}, nm	$\Delta\lambda_{1/2}$, nm	$N, \cdot 10^{22}$ cm^{-3}	$\gamma, \cdot 10^{15}$ s^{-1}
Aqueous solution Ag	20	416	45	7,46	3,64
Aqueous solution Ag-TiO$_2$ (concentration of TIPT 30 %)	43	420	62	7,35	3,04
Aqueous solution Ag-TiO$_2$ (concentration of TIPT 50 %)	84	424	58	7,20	3,86
Ethanol solution Ag	50	407	65	-	-
Ethanol solution Ag-TiO$_2$	130	-	-	-	-

Electron-microscopic studies of NPs and NSs showed that they are predominantly spherical in shape and correspond to the results obtained in [9]. The Ag NPs and Ag-TiO$_2$ NSs in ethanol were also synthesized. The main characteristics of the obtained NPs and NSs are shown in Table.

The absorption spectra of silver NPs and Ag-TiO$_2$ NSs in ethanol and aqueous solutions are shown in Figure 3. It is seen from the figure that the maximum plasmon resonance of silver NPs is in the range 410–415 nm (curve 1). The absorption spectra of the NSs solutions are observed. As it is known, the absorption band of TiO$_2$ is located in the ultraviolet part of the spectrum, starting at 360 nm. Therefore, the change in the absorption spectrum is due to the formation of TiO$_2$ particles in a solution with silver NPs. With an increase of shell thickness in NSs from 23 nm (curve 2) to 63 nm (curve 3) a significant decrease in the intensity of the plasmon resonance band of NPs in aqueous solution occurs (Fig. 3, a). The formation of the TiO$_2$ semiconductor shell is indicated by a decrease in the intensity of the plasmon resonance of silver NPs and the red–shift of its maximum. A similar result was obtained for the absorption spectra of NPs and NSs in ethanol (Fig. 3, b).
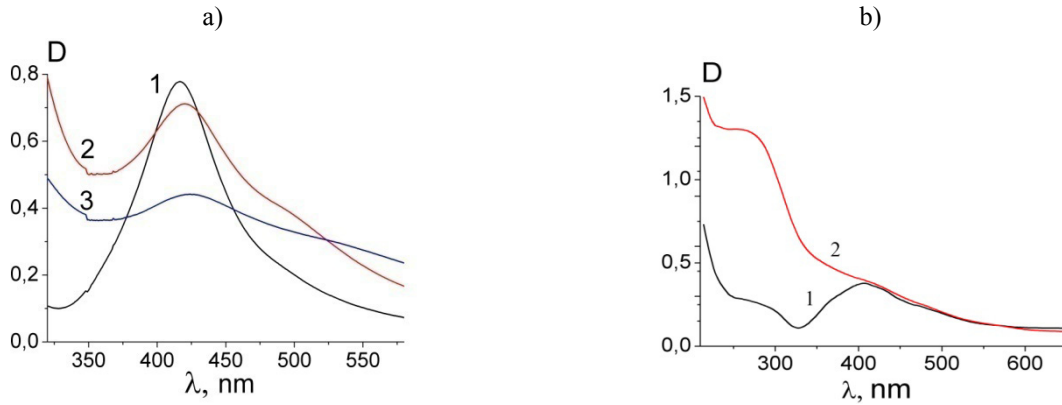
Figure 3. Absorption spectra of the Ag (1) and Ag-TiO$_2$ (2, 3) with
r_{shell}=23 nm (2) and r_{shell}=63 nm (3) in aqueous (a) and ethanol (b) solutions

For spherical NPs, the frequency (ω) corresponding to the maximum of the absorption spectrum is related to the plasmon resonance frequency (ω$_p$) by the following formula:

$$\omega = \frac{\omega_p}{\sqrt{3}}. \tag{1}$$

The half–width of the absorption spectrum is also one of the main characteristics of plasmon resonance. It carries information on the distribution of LPR by size. The values λ_{abs}^{max} and $\Delta\lambda 1/2$ contain information on the relaxation of plasmon oscillations, electron density, and other characteristics of LPR. Thus, knowledge of the maximum of the absorption spectrum and the shape of NPs makes it possible to determine the frequency of plasmon resonance of NPs and a number of important parameters characterizing the properties of LPR.

For metals NPs, the position of the plasmon absorption band can be described by the following formulas [11, 12]:

$$\lambda_{peak}^2 = \lambda_p^2 (\varepsilon^\infty + 2\varepsilon_m) \tag{2}$$

$$\lambda_p^2 = 4\pi^2 c^2 m \varepsilon_0 / Ne^2, \tag{3}$$

where, λ_p^2 is the volume plasma wavelength in terms of the electron mass, ε_0 is the vacuum dielectric constant, e is the charge of the electron, and N is the electron density in the particle; ε^∞ is the high–frequency dielectric constant (for silver – about 4,9 ± 0,3, for gold – 6,9 [13]) ε_m is the numerical value equivalent to the square of the refractive index of the solvent. For ethyl alcohol, ε_m was taken equal to 3,7 [9].

In the formation of a shell of titanium dioxide on the surface of NPs, the electron density N will decrease. This, in turn, will lead to an increase in λ_p^2 (formula 3). This is expressed in the long–wavelength shift of the maximum of the LPR. A decrease in the electron density N will lead to a decrease in the absorption intensity of the LPR, which is observed in Figure 3. These results show that the formation of the TiO$_2$ film occurs on the surface of the Ag NPs.

As shown in [11, 12], under the condition that the radius is lower than the wavelength of the incident radiation, a linear dependence of the form is applicable:

$$\frac{1}{k} = \frac{\theta_2}{\theta_1} + \frac{1}{\theta_1}\left(\frac{\lambda_{peak}^2}{\lambda} - \lambda\right)^2. \tag{4}$$

From the graph of the dependence of $\frac{1}{k}$ on $\left(\dfrac{\lambda_{peak}^2}{\lambda} - \lambda\right)^2$, the parameters of the linear dependence

(formula 4) θ_1 and θ_2 were determined. Figure 4 shows the dependence of $\frac{1}{k}$ on $\left(\dfrac{\lambda_{peak}^2}{\lambda} - \lambda\right)^2$ for solutions

of silver NPs and NSs Ag-TiO$_2$. Using the parameters θ_1 and θ_2, the attenuation coefficient of plasma oscillations γ was determined by the formula:

$$\gamma = \frac{2\pi c\, \theta_2^{1/2}}{\lambda_{peak}^{2}}$$

(5)
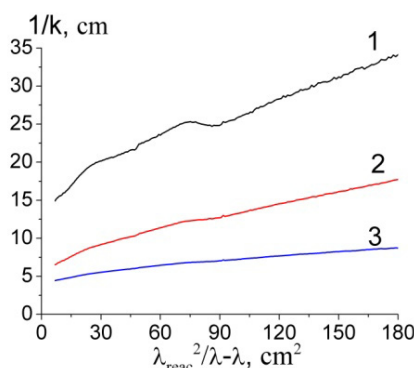
Figure 4. Dependence of 1/k on λ for a colloidal solution of silver
NPs (1) and Ag-TiO$_2$ NSs (2,3) with r$_{shell}$=23 nm (2) and r$_{shell}$=63 nm (3)

The electron density N (formula 3) and the damping coefficient of plasma oscillations γ are given in Table. From the data in the table it can be seen that during the formation of the TiO$_2$ semiconductor shell, the concentration of electrons participating in the formation of LPR in silver decreases. This indicates deterioration in the quality of LPR in plasmon NPs when depositing a semiconductor shell on them. The rate of damping of plasma oscillations varies in different ways depending on the thickness of the TiO$_2$ shell. At small thicknesses of TiO$_2$, the rate of damping of plasma oscillations decreases. This can be seen both in the results given in Table and in [9]. With increasing shell thickness, the value of γ for Ag-TiO$_2$ (r$_{shell}$=63 nm) increases. This leads to an increase in the damping plasma of plasma oscillations. In the case of NPs obtained in ethanol, the above calculation algorithm could not be used due to the inability to determine the value λ_{abs}^{max} from the absorption spectrum of the obtained NS (Fig. 3, b, curve 2).

Titanium dioxide NPs have their own luminescence [8, 14]. However, because the luminescence occurs with indirect optical transitions of an electron, the intensity of the glow is quite low. Figure 5 (a) shows the luminescence spectra of ethanol solutions of TiO$_2$ NPs and Ag-TiO$_2$ NSs. The excitation was carried out by ultraviolet radiation with λ_{excit}=300 nm. The concentration of TiO$_2$ NPs and Ag-TiO$_2$ NSs was chosen in such a way that the optical absorption of TiO$_2$ remained unchanged. The size of silver NPs was 50 nm. It can be seen from Figure 6 (a) that the luminescence spectra of Ag-TiO$_2$ nanostructures are significantly different from the TiO$_2$ luminescence spectra. In the luminescence spectrum of Ag-TiO$_2$, a new band appears with a maximum at 575 nm. This corresponds to the energy of 2,16 eV. This band was registered by the authors of [8] and is explained by them as the luminescence of silver NPs during charge transfer from TiO$_2$ to silver. The luminescence intensity of Ag-TiO$_2$ is much lower than the luminescence intensity of TiO$_2$, which is also explained by the transfer of electrons from the conduction band of titanium dioxide to the conduction band of silver NPs.

In the case of an aqueous solution of Ag and Ag-TiO$_2$ NPs, the luminescence of Ag NPs was recorded (Fig. 5, b). For silver NPs, luminescence can be observed [15, 16] if their size is sufficiently small. This luminescence is explained by the emission of small silver clusters [15]. An additional luminescence band with a maximum at 540 nm appears in the luminescence spectrum for an aqueous solution of Ag-TiO$_2$ NSs, as for an ethanol solution of Ag-TiO$_2$ NSs (Fig. 5 b, curve 2, 3).

a)

b)

1 –TiO$_2$ NPs; 2 – Ag-TiO$_2$

1 –Ag NPs; 2 – Ag-TiO$_2$ with r_{shell}=23 nm; 3 – Ag-TiO$_2$ with r_{shell}=63 nm
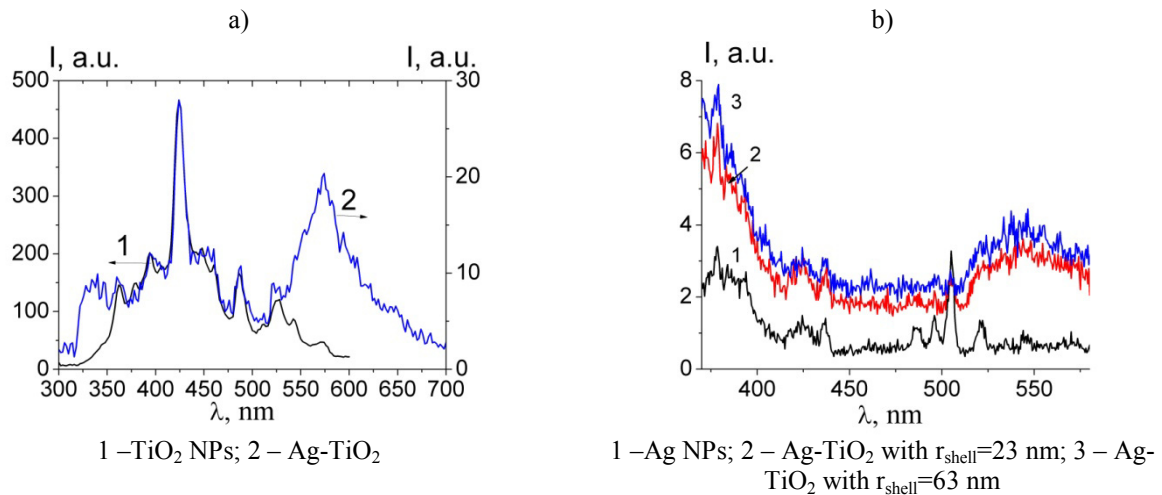
Figure 5. Luminescence spectra of solutions of Ag, TiO$_2$ and Ag-TiO$_2$ in ethanol (a) and in water (b)

A possible mechanism of charge transfer is described in [9] and is shown in Figure 5. In the first stage of the process, the light quantum of TiO$_2$ is absorbed and the electron is transferred from the conduction band of TiO$_2$ to the Fermi level (E_F) of the metal NPs (Fig. 6, a). In the second stage, the electron returns from the Fermi level to the valence band of the semiconductor (E_v). In this case, recombination luminescence with the wavelength of the corresponding transition energy $\Delta E = E_F – E_v$ can occur (Fig. 6, b). The value of ΔE for the transition between the Fermi level of the solid body of Ag and Au and the valence band of TiO$_2$ is 2,9 eV [17]. At the same time, as shown in [18], the Fermi level of gold NPs can vary from the value observed for atomic gold of 9,2 eV to a value corresponding to a bulk material (5,3 eV). However, the value of the Fermi level depends both on the size and on the charge of the NPs [16].

The transfer energy ΔE from the Fermi level is 2,3 eV. At the same time, the increase in the thickness of the TiO$_2$ shell from 23 nm to 63 nm does not lead to a significant increase in luminescence with a maximum at 540 nm or a shift in the maximum of the luminescence band at 540 nm. This suggests that the luminescence at 540 nm is formed by transferring a charge from a layer of titanium dioxide bordering on silver. In this case, the thickness of the TiO$_2$ shell does not have a large effect on the value of ΔE. Therefore, the outlying TiO$_2$ layer from the silver does not participate in the charge transfer process. In the luminescence spectrum of aqueous solutions of Ag-TiO$_2$ NSs, no luminescence of TiO$_2$ is observed. Perhaps this is due to the low value of the quantum yield of the luminescence of TiO$_2$ in comparison with the luminescence of Ag clusters.

As shown in [18], the value of the Fermi level (E_F) depends both on the size and on the charge of the low frequency. The decrease in the value of E_F should occur with a decrease in the size of the NPs. In our case, the value of ΔE increases with decreasing size of the low frequency. Silver NPs with a diameter of 50 nm have $\Delta E = 2,16$ eV, silver NPs with a diameter of 20 nm have $\Delta E = 2,3$ eV. The observed values of ΔE for different Ag-TiO$_2$ NSs are related to the charge value for silver NPs. At the NPs with d=20 nm, a more negative charge should be presented compared to the NPs with d = 50 nm.

a)

b)
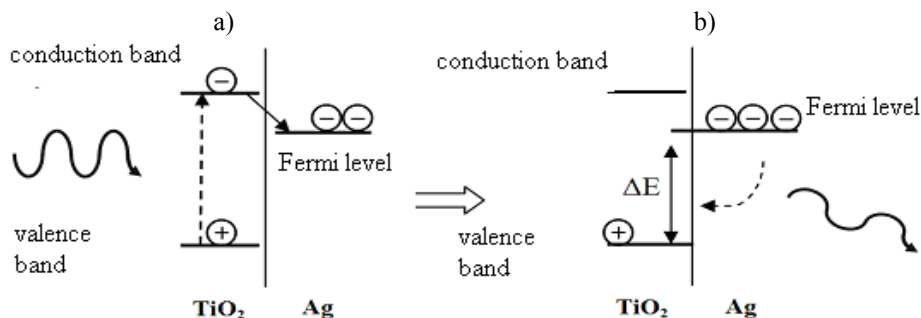
Figure 6. Mechanism of charge transfer and luminescence in the Ag-TiO$_2$ NSs

Thus, the paper presents the results of the synthesis of Ag-TiO$_2$ nanostructures. Measurement of the size and shape of the obtained NSs. The size of the NSs was determined using the method of dynamic light scattering. When using the absorption spectra of solutions of NPs and NSs, the electron density and attenuation coefficient of plasma oscillations γ were determined. It is shown that the TiO$_2$ semiconductor shell reduces the electron density concentration of plasmon NPs. In this case, the damping rate of plasma oscillations varies in different ways and depends on the thickness of the synthesized shell. With a small thickness (r_{shell}=23 nm), the decay rate decreases. With a large shell thickness (r_{shell}=63 nm), the oscillation damping rate γ increases. The obtained results show that the quantitative indicator of NPs in NSs (electron density) is deteriorating, while the qualitative indicator of LPR (attenuation coefficient of plasma oscillations) can improve in the case of a thin TiO$_2$ shell (r_{shell}=23 nm). Also, after the synthesis of the TiO$_2$ shell, an additional luminescence band of the Ag-TiO$_2$ NSs occurs. This luminescence is associated with charge transfer from TiO$_2$ to Ag. The dependence of the maximum recombination luminescence band on the value of the charge on silver NPs is observed.

References

1   Ghosh R. Core/Shell Nanoparticles: Classes, Properties, Synthesis Mechanisms, Characterization, and Applications / Ch.Paria, S.Paria // Chemical Reviews, — 2012. — 112. — P. 2373–2433.

2   Рыжонков Д.И. Наноматериалы / Д.И. Рыжонков, В.В. Лёвина, Э.Л. Дзидзигури. — 2–е изд. — М.: БИНОМ; Лаборатория знаний, 2010. — 365 с.

3   Зимон А.Д. Коллоидная химия НЧ / А.Д. Зимон, А.Н. Павлов. — М.: Научный мир, 2012. — 224 с.

4   Yin X. Ag/TiO2 nanocomposites with improved photocatalytic properties prepared by a low temperature process in polyethylene glycol / Que W., Y. Liao // Colloids and surf. A: Physicochem. eng. Aspects, — 2012. — 410. — P. 153–158.

5   Qi J. Highly efficient plasmon–enhanced dye–sensitized solar cells through metal@oxide core–shell Nanostructure / J. Qi, X. Dang, P.T. Hammond, A.M. Belcher // ACS Nano. — 2011. — 5, 9. — P. 7108–7116.

6   Zhang R. Influence of SiO2 shell thickness on power conversion efficiency in plasmonic polymer solar cells with Au nanorod@SiO2 core–shell structures / R. Zhang, Y. Zhou, L. Peng // Scientific Reports. — 2016. — 6, 25036. — P. 1–9.

7   Clavero C. Plasmon-induced hot-electron generation at nanoparticle/metal-oxide interfaces for photovoltaic and photocatalytic devices / C. Clavero // Nature Photonics. — 2014. — 8. — P. 95–103.

8   Calandra P. Structural and optical properties of novel surfactant coated TiO2–Ag based nanoparticles / P. Calandra, A. Ruggirello, A. Pistone, V.T.J. Liveri // Clust. Sci. — 2010. — 21. — P. 767–778.

9   Afanasyev D.A. Effect of the titanium dioxide shell on the plasmon properties of silver nanoparticles / D.A. Afanasyev, N.Kh. Ibrayev, T.M. Serikov, A.K. Zeinidenov // Russian Journal of Physical Chemistry. — 2016. — 90. — 4. — P. 833–837.

10 Afanasyev D.A. Synthesis of aluminum-aluminium oxide nanostructures by laser ablation / D.A. Afanasyev, N.Kh. Ibrayev, M.E. Kasymov // Bulletin of the Karaganda University, physics series. — 2018. — 3, 91. — P. 8–15.

11 Toporko, A.V. Change of the properties of copper small particles during sulfur-containing ions adsorption from solutions / A.V. Toporko, V.V. Tsvetkov, V.D. Yagodovskii, A. Issa // Zhurnal fizicheskoi khimii. — 1995. — 5, 69. — P. 867–870.

12 Подлегаева Н.Л. Исследование свойств НЧ серебра, полученных восстановлением из растворов и термическим напылением в вакууме / Н.Л. Подлегаева, Д.М. Руссаков, С.А. Созинов, Т.В. Морозова, И.Л. Швайко, Н.С. Звиденцова, Л.В.Колесников // Вестн. Кемер гос. ун-та. Сер. Химия. — 2009. — № 2. — С. 95–99.

13 Shklyarevskii I.N. Separation of the contribution of free and bound electrons into real and imaginary parts of the dielectric constant of gold / I.N. Shklyarevskii, P.L. Pakhmov // Optika i Spektroskopia. — 1973. — 34, 1. — P. 163–166.

14 Serpone N. Size Effects on the Photophysical Properties of Colloidal Anatase Ti0$_2$ Particles: Size Quantization or Direct Transitions in This Indirect Semiconductor / N. Serpone, D. Lawless, R.J. Khairutdinov // Phys. Chem. — 1995. — 99, 16646–16654.

15 Bulavchenko, A.I. Photon correlation spectroscopic and spectrophotometric studies of the formation of cadmium sulfide nanoparticles in ammonia-thiourea solutions / A.I. Bulavchenko, A.N. Kolodin, T.Yu. Podlipskaya, M.G. Demidova, E.A. Maksimovskii, N.F. Beizel', S.V. Larionov, A.V. Okotrub // Russian Journal of Physical Chemistry A. — 2015. — 90, 5, 1034–1038.

16 Ping H. Photoluminescence phenomenon during the formation of silver nanoparticles / H. Ping, Sh. Xing–Hai, G. Hong–Cheng // Acta Phys. Chim. Sin. — 2004. — 20, 10, 1200–1203.

17 Kasap S.O. Principles of Electronic Materials and Devices, Third Edition McGraw–Hill, 2002. 768 p.

18 Scanlon M.D. Charging and discharging at the nanoscale: Fermi level equilibration of metallic nanoparticles / M.D. Scanlon, P. Peljo, M.A. Méndez, E. Smirnov, H.H. Girault // Chem. Sci, 2015. 6, 5, 2705–2720.

Д.А. Афанасьев, Н.Х. Ибраев, Э.Ж. Алихайдарова

Ag–TiO₂ нанокұрылымдарында зарядты тасымалдау және локалды плазмондық резонанс қасиеттері

Мақалада Ag–TiO₂ нанокұрылымдары синтезінің нәтижелері келтірілген. Нанокұрылымдар күміс ядросынан және TiO₂ жартылайөткізгіш қабыршағынан тұрады. Қолданылған еріткіштің тәуелділігіне байланысты жарықтың динамикалық шашырау әдісімен анықталған нанокұрылымдардың (НҚ) өлшемі 20 нм және 50 нм құрады. TiO₂ жартылайөткізгіш қабыршағының күміс нанобөлшектерінің локалды плазмондық резонанс қасиеттеріне әсері зерттелді. НҚ-да локалды плазмондық резонанстың сандық көрсеткіші (электрондық тығыздығы) нашарлайды, алайда локалды плазмондық резонанстың сапалық көрсеткіші (плазмалық тербелістердің өшу коэффициенті) TiO₂ қабықшасы жұқа болғанда жақсаратыны дәлелденді. Сонымен қатар TiO₂ қабықшасының синтезінен кейін Ag-TiO₂ НҚ-да люминесценцияның қосымша жолағы байқалды. Бақыланатын жарқырау TiO₂-ден Ag-ға зарядтың тасымалдалуына байланысты болып табылады. Күміс НБ-де зарядтың мәніне тәуелді рекомбинациялық люминесценция жолағының максимумы байқалды.

Кілт сөздер: локалды плазмондық резонанс, күміс нанобөлшектері, нанокұрылымдар, заряд тасымалдау, титан диоксиді.

Д.А. Афанасьев, Н.Х. Ибраев, Э.Ж. Алихайдарова

Перенос заряда и свойства локализованного плазмонного резонанса в наноструктурах Ag–TiO₂

В статье приведены результаты синтеза наноструктур Ag–TiO₂. Наноструктуры состоят из серебряного ядра и полупроводниковой оболочки TiO₂. Размер наноструктур (НС), определенный методом динамического рассеяния света, составил 20 нм и 50 нм в зависимости от использованного растворителя. Исследовано влияние полупроводниковой оболочки TiO₂ на свойства локализованного плазмонного резонанса наночастиц серебра. Установлено, что количественный показатель локализованного плазмонного резонанса в НС (электронная плотность) ухудшается, в то время как качественный показатель локализованного плазмонного резонанса (коэффициент затухания плазменных колебаний) может улучшиться в случае тонкой оболочки TiO₂. Также после синтеза оболочки TiO₂ наблюдается дополнительная полоса люминесценции НС Ag-TiO₂. Наблюдаемое свечение связано с переносом заряда с TiO₂ на Ag. Наблюдается зависимость максимума полосы рекомбинационной люминесценции от значения заряда на НЧ серебра.

Ключевые слова: локализованный плазмонный резонанс, наночастица серебра, наноструктуры, перенос заряда, диоксид титана.

References

1 Ghosh R., Paria Ch., & Paria S. (2012). Core/Shell Nanoparticles: Classes, Properties, Synthesis Mechanisms, Characterization, and Applications. *Chemical Reviews*, 112, 2373–2433.

2 Ryzhonkov, D.I., Levina, V.V., & Dzidziguri, E.L. (2010) *Nanomaterialy [Nanomaterials]*. Moscow: BINOM; Laboratoriia znanii [in Russian].

3 Zimon, A.D., & Pavlov, A.N. (2012) *Kolloidnaia himiia nanochastits [Colloid chemistry of nanoparticles]*. Moscow: Nauchnyi mir [in Russian].

4 Yin X., Que W., & Liao Y. (2012). Ag/TiO₂ nanocomposites with improved photocatalytic properties prepared by a low temperature process in polyethylene glycol. Colloids *and surf. A: Physicochem. eng. Aspects*, 410, 153–158.

5 Qi J., Dang X., Hammond P.T., & Belcher A.M. (2011). Highly efficient plasmon–enhanced dye–sensitized solar cells through metal@oxide core–shell Nanostructure. *ACS Nano*, 5, 9, 7108–7116.

6 Zhang R., Zhou Y., & Peng L. (2016). Influence of SiO2 shell thickness on power conversion efficiency in plasmonic polymer solar cells with Au nanorod@SiO₂ core–shell structures. *Scientific Reports*, 6, 25036, 1–9

7 Clavero C. (2014). Plasmon-induced hot-electron generation at nanoparticle/metal-oxide interfaces for photovoltaic and photocatalytic devices. *Nature Photonics*, 8, 95–103.

8 Calandra P., Ruggirello A., Pistone A., & Liveri V.T. (2010). Structural and optical properties of novel surfactant coated TiO2–Ag based nanoparticles. *J. Clust. Sci*, 21, 767–778.

9 Afanasyev, D.A., Ibrayev, N.Kh., Serikov, T.M., & Zeinidenov, A.K. (2016) Effect of the titanium dioxide shell on the plasmon properties of silver nanoparticles. *Russian Journal of Physical Chemistry* 90, 4, 833–837.

10 Afanasyev, D.A., Ibrayev, N.Kh., & Kasymov, M.E. (2018). Synthesis of aluminum-aluminium oxide nanostructures by laser ablation. *Bulletin of the Karaganda University, Physics series,* 3, 91, 8–15.

11 Toporko, A.V., Tsvetkov, V.V., Yagodovskii, V.D., & Issa, A. (1995). Change of the properties of copper small particles during sulfur-containing ions adsorption from solutions. *Zhurnal fizicheskoi khimii,* 5, 69, 867–870.

12 Podlegaeva, N.L., Russakov, D.M., Sozinov, S.A., Morozova, T.V., Shvaiko, I.L. Zvidencova, N.S., & Kolesnikov, L.V. (2009). Issledovanie svoistv nanochastic serebra, poluchennykh vosstanovleniem iz rastvorov i termicheskim napyleniem v vakuume [Investigation of the properties of silver nanoparticles obtained by reduction from solutions and thermal spraying in vacuum]. *Vestnik Kemerovskoho hosudarstvennoho universiteta. Seriia Himiia – Bulletin of Kemerovo State Universit. Chemistry, Vol. 2,* 95–99 [in Russian].

13 Shklyarevskii, I.N., & Pakhmov P.L. (1973). Separation of the contribution of free and bound electrons into real and imaginary parts of the dielectric constant of gold. *Optika i Spektroskopiya,* 34, 1, P. 163–166.

14 Serpone N., Lawless D., & Khairutdinov R. (1995). Size Effects on the Photophysical Properties of Colloidal Anatase TiO_2 Particles: Size Quantization or Direct Transitions in This Indirect Semiconductor. *J. Phys. Chem,* 99, 16646–16654.

15 Bulavchenko, A.I., Kolodin, A. N., Podlipskaya, T.Yu., Demidova, M.G., Maksimovskii, E.A., Beizel', N.F., Larionov, S.V., & Okotrub, A.V. (2015). Photon correlation spectroscopic and spectrophotometric studies of the formation of cadmium sulfide nanoparticles in ammonia-thiourea solutions. *Russian Journal of Physical Chemistry A*, 90, 5, 1034–1038.

16 Ping H., Xing–Hai Sh., & Hong–Cheng G. (2004). Photoluminescence phenomenon during the formation of silver nanoparticles. *Acta Phys. — Chim. Sin,* 20, 10, 1200–1203.

17 Kasap S.O. (2002). Principles of Electronic Materials and Devices, Third Edition. McGraw–Hill, 768 p.

18 Scanlon M.D., Peljo P., Méndez M.A., Smirnov E., & Girault H.H. (2015). Charging and discharging at the nanoscale: Fermi level equilibration of metallic nanoparticles. *Chem. Sci,* 6, 5, 2705–2720.